

Room-temperature Coulomb-blockade-dominated transport in gold nanocluster structures

L Clarke[†], M N Wybourne[‡], L O Brown[§], J E Hutchison[§],
M Yan[§], S X Cai[§] and J F W Keana[§]

[†] Department of Physics, University of Oregon, Eugene, OR 97403, USA

[‡] Department of Physics and Astronomy, Dartmouth College, Hanover, NH 03755, USA

[§] Department of Chemistry, University of Oregon, Eugene, OR 97403, USA

Received 7 December 1997, accepted for publication 11 March 1998

Abstract. In this paper we discuss the near-room-temperature electrical transport characteristics of structures made from ligand-stabilized metal clusters. The structures show threshold behaviour, nonlinear current–voltage characteristics and radio-frequency-induced plateaux consistent with Coulomb-blockade-dominated transport in disordered arrays of metal dots. Samples having triphenylphosphine and octadecanethiol ligand shells are found to have a 3 orders of magnitude difference in current above threshold. We discuss a possible explanation for this observation.

1. Introduction

One single-electron phenomenon that can be understood from classical electrostatics is the Coulomb-blockade effect in metal systems. For a metallic object of capacitance C , the energy associated with the transfer of one electron from a reservoir to the object is $E_C = e^2/2C$. When this energy is large compared with the available thermal energy, kT , and the tunnel resistance between the object and its surroundings, R_T , is much greater than the quantum resistance h/e^2 , the transport properties of the system become strongly influenced by the discrete nature of the electron charge. Coulomb-blockade effects have been observed at room temperature in very-low-capacitance semiconductor devices [1]. A metallic system that offers both the small capacitance and the resistive isolation needed for room-temperature Coulomb blockade is ligand-stabilized metal clusters that contain a small number of atoms [2–5].

One nanocluster that has received particular attention is dodeca(triphenylphosphine)hexa(chloro)pentaconta gold, $\text{Au}_{55}[\text{P}(\text{C}_6\text{H}_5)_3]_{12}\text{Cl}_6$. This cluster has a metal core diameter of 1.4 nm and a total diameter of 2.1 nm [2]. Using the classical expression for capacitance of an isolated conducting sphere, $C = 4\pi\epsilon\epsilon_0r$, with a dielectric constant $\epsilon < 5$ the Coulomb charging energy of the Au_{55} core is estimated to be much greater than kT at room temperature. Furthermore, the ligand shell is expected to meet the requirement that $R_T \gg h/e^2$.

A useful feature of ligand-stabilized nanoclusters is the lability of the ligand shell, which may be used to tailor transport properties of the system [6]. For instance, when exposed to octadecanethiol ($\text{SC}_{18}\text{H}_{37}$) groups, the $[\text{P}(\text{C}_6\text{H}_5)_3]_{12}\text{Cl}_6$ ligand shell undergoes substitution to form a cluster with approximately 20 stabilizing thiol ligands. Investigations have shown the octadecanethiol stabilized cluster to be more stable in solution, and thus it may provide a more robust platform for room-temperature Coulomb-blockade structures [6].

In this paper we report the transport characteristics of $\text{Au}_{55}[\text{P}(\text{C}_6\text{H}_5)_3]_{12}\text{Cl}_6$ and octadecanethiol-stabilized Au_{55} . We present data on two different sample configurations. In the first, electron-beam lithography is used to delineate the samples [7], while in the second a solution containing the clusters is drop cast on a prefabricated electrode array. In both methods we observe nonlinear current–voltage (I – V) characteristics near room temperature that are consistent with Coulomb-blockade-dominated transport. We also present data showing the response of the direct-current (DC) I – V characteristic to the application of an external RF signal.

2. Experiment

The $\text{Au}_{55}[\text{P}(\text{C}_6\text{H}_5)_3]_{12}\text{Cl}_6$ material was synthesized using the Schmid procedure [8] and purified to remove monomer material. Thin films for the first type of sample were

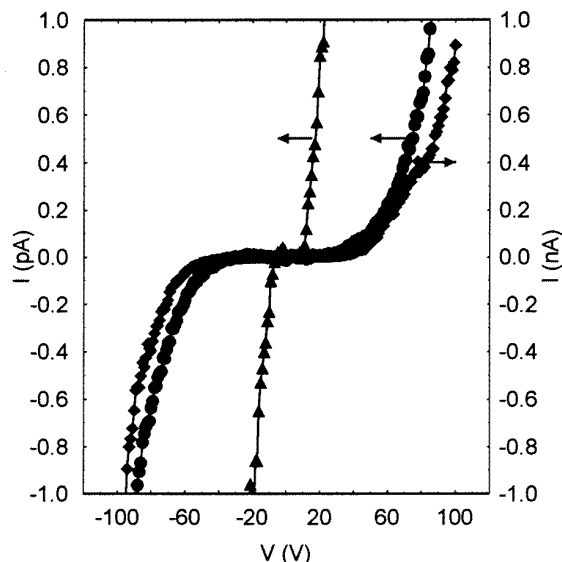


Figure 1. Current–voltage characteristics of patterned \blacktriangle and non-patterned \bullet $\text{Au}_{55}[\text{P}(\text{C}_6\text{H}_5)_3]_{12}\text{Cl}_6$ clusters and octadecanethiol-stabilized Au_{55} clusters (\blacklozenge). The patterned sample was measured at 195 K; the other two were measured at 295 K.

produced on Si_3N_4 as described elsewhere [4]. Exposure to a 40 kV electron beam with a line dosage of 100 nC cm^{-1} followed by development in dichloromethane produced well-defined structures with dimensions as small as $0.1 \mu\text{m}$. Atomic force microscopy measurements determined the thickness of the structures to be 50 nm. Gold contacts to the patterned samples were fabricated using conventional electron beam lithography, lift-off and thermal evaporation. Non-patterned $\text{Au}_{55}[\text{P}(\text{C}_6\text{H}_5)_3]_{12}\text{Cl}_6$ samples were fabricated by drop casting onto interdigitated gold electrodes on glass. The individual electrode width and separation were $15 \mu\text{m}$. Octadecanethiol-stabilized clusters were synthesized as described elsewhere [6]. Non-patterned samples suitable for electrical measurement were made by drop casting this material onto interdigitated electrodes on glass.

Electrical measurements were made under vacuum in a shielded vessel that was temperature regulated from 195 to 350 K. The samples were mounted on a clean Teflon stage and connected to a DC voltage source and electrometer with rigid triaxial lines. The background leakage current of the apparatus set the minimum resolvable conductance at about $10^{-15} \Omega^{-1}$. For each measurement, a control experiment was performed to determine the leakage current of the apparatus and sample holder. The I – V characteristics were obtained by correcting for the intrinsic leakage. Constant-amplitude RF signals with frequencies in the range 0.1–5 MHz were applied to some samples via a dipole antenna. The RF coupling between antenna and the sample was not optimized.

3. Results and discussion

Both patterned and non-patterned triphenylphosphine-stabilized samples exhibited highly nonlinear I – V

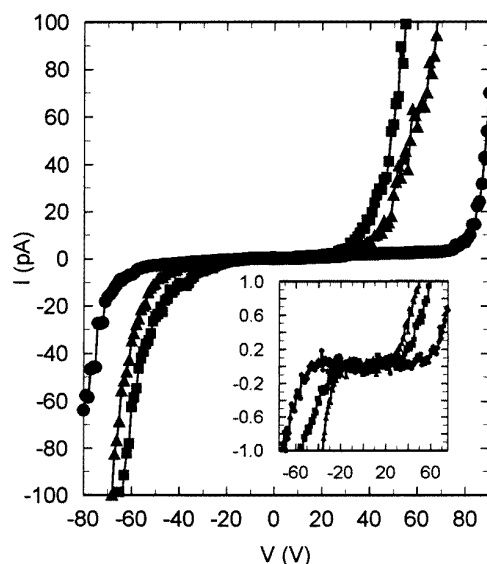


Figure 2. Threshold voltage shift as a function of voltage sweep for the non-patterned octadecanethiol-stabilized Au_{55} clusters. The inset shows the behaviour for the $\text{Au}_{55}[\text{P}(\text{C}_6\text{H}_5)_3]_{12}\text{Cl}_6$ clusters. The current scale for the inset is $\times 10^{-13}$ A. Both samples were measured at 295 K.

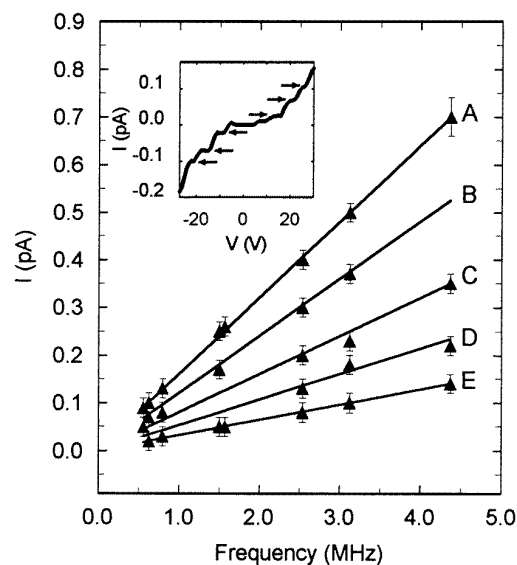


Figure 3. Current values of the observed plateaux as a function of applied radio frequency measured in the patterned $\text{Au}_{55}[\text{P}(\text{C}_6\text{H}_5)_3]_{12}\text{Cl}_6$ clusters at 195 K. The full lines have slopes (A) e , (B) $3e/4$, (C) $e/2$, (D) $e/3$ and (E) $e/5$, where $e = 1.6 \times 10^{-19}$ C. The inset is the plateau structure at $f = 0.626$ MHz. The arrows indicate the plateau positions.

behaviour, as shown in figure 1. For the patterned sample, clear blockade was seen at 195 K with current suppression up to a threshold voltage of magnitude 6.7 ± 0.6 V. For the non-patterned sample, the blockade behaviour was seen at 295 K. The threshold voltage in the non-patterned samples decreased as a function of the time under bias, as illustrated in the inset to figure 2. Threshold behaviour was also seen in the octadecanethiol sample at 295 K, as

shown in figure 1. The currents above threshold were much larger than observed in the patterned and non-patterned triphenylphosphine samples. The size of the threshold voltage in the octadecanethiol systems also decreased as a function of time bias was applied, as seen in figure 2. RF signals introduced constant-current plateaux in the I - V characteristics of all samples; however, the threshold instability of the drop-cast samples prevented a detailed study of this effect. A characteristic plateau structure in a patterned $\text{Au}_{55}[\text{P}(\text{C}_6\text{H}_5)_3]_{12}\text{Cl}_6$ sample is shown in the inset to figure 3. The current at which the plateaux occur is proportional to the applied signal frequency. Several constants of proportionality were observed with the largest being $1.59 \pm 0.04 \times 10^{-19}$ C. A plot of observed current position of the plateau versus applied frequency is shown in figure 3.

Several groups have modelled the transport behaviour of ordered and disordered one- and two-dimensional arrays of metal dots [9–12]. As discussed previously [4], the Middleton and Wingreen (MW) model of a disordered array of normal metal dots best describes our data. In this model the threshold voltage, V_T , scales with the number of junctions between source and drain, and above threshold the current is predicted to scale as $I \sim (V/V_T - 1)^\gamma$. Analytically, γ is 1 for one-dimensional arrays and $5/3$ for infinite two-dimensional arrays. Numerical simulations find $\gamma = 2.0 \pm 0.2$ for finite two-dimensional arrays. In all three types of samples, the I - V characteristics above threshold scaled as predicted by MW. For the triphenylphosphine-stabilized clusters, $\gamma = 1.6 \pm 0.2$ and 2.1 ± 0.3 , for the patterned and non-patterned cases respectively. We interpret these values to indicate that the non-patterned samples are two dimensional while the patterned samples fall somewhere between the one- and two-dimensional regimes. For octadecanethiol-stabilized clusters $\gamma = 2.6 \pm 0.3$. This value falls outside the range predicted by MW and may indicate that the samples have a dimensionality greater than 2. For both types of cluster, the threshold voltages obtained from scaling were consistent with those estimated directly from the data.

The RF-induced response in the triphenylphosphine-patterned samples is similar to that reported in one-dimensional systems [13,14]. The effect is caused by phase locking of single-electron tunnelling events and the applied RF signal [15]. In principle, phase locking is possible in two-dimensional arrays but could be quite sensitive to inhomogeneity. However, in the case of a very inhomogeneous two-dimensional array with only a single or few percolation paths the one-dimensional description should apply. Phase locking occurs when the n th harmonic of the applied frequency, f , corresponds to the m th harmonic of the frequency of tunnelling in the system. Then the current becomes locked and plateaux are seen at $I = (n/m)ef$. Fits to the data occur for rational fractions, n/m , of $1/5$, $1/3$, $1/2$, $3/4$ and 1 , as seen in figure 3. Thus, the RF response supports the hypothesis that correlated tunnelling occurs in the samples. By studying the activated behaviour of the current in the Coulomb gap [4], we have argued that transport is dominated by the charging of single Au_{55} cores.

Two differences between the patterned and non-patterned triphenylphosphine samples are the long-term stability of the transport characteristics and the temperature at which clear blockade is seen. The increased stability of the patterned sample is probably the result of a more rigid structure created by the electron-beam irradiation. Such irradiation may crosslink the ligand spheres, thereby locking the metal cores in place. The irradiation seems to lower the characteristic charging energy of the system as evidenced by measurable conduction below the threshold at 295 K. In the case of the non-patterned samples, both triphenylphosphine- and octadecanethiol-stabilized clusters show clear blockade behaviour at 295 K. Thus, another consequence of the crosslinking appears to be an increase in the capacitance of the clusters within the array.

The major difference between the non-patterned triphenylphosphine- and octadecanethiol-stabilized cluster arrays is the magnitude of the current above threshold, as seen in figure 1. Currents observed in the octadecanethiol samples are about 3 orders of magnitude greater than in either type of triphenylphosphine sample although the threshold voltages and the decrease in threshold voltage with measurement are similar in the two materials. The current magnitude is expected to be inversely proportional to the tunnel resistance and proportional to the number of parallel current paths [12]. Therefore, the increased current could be the result of either a lower tunnel resistance or a greater number of paths, or a combination of both effects. The larger γ in the octadecanethiol material may result from higher dimensionality, which is consistent with additional current paths, and thus higher current magnitudes. An effect that could influence both the tunnelling resistance and the dimensionality of the system is the interdigitation of the octadecanethiol chains to form small, three-dimensional aggregates. Some evidence for this mechanism comes from the fact that solutions can only be formed with the addition of heat. Also, unlike the triphenylphosphine samples, when attempts are made redissolve the octadecanethiol samples aggregation is observed. Further work is in progress to determine whether interdigitation is responsible for the enhanced current magnitude in the octadecanethiol-stabilized material.

4. Conclusion

By investigating the current-voltage and RF response of triphenylphosphine and octadecanethiol ligand stabilized gold clusters, we have shown that single-electron effects dominate the near-room-temperature transport. Samples patterned by electron-beam lithography have increased stability over non-patterned samples. We believe that this increased stability is the result of crosslinking between ligand shells which tends to lock the gold clusters in place. We have also found the different ligand shells studied show significantly different currents above threshold. One suggested mechanism for this increase is that the long-chain ligands allow interdigitation which may increase the dimensionality of the sample.

Acknowledgment

This work was supported in part by the Office of Naval research under Contracts N00014-93-0618 and N00014-93-1-1120.

References

- [1] Yano K, Ishii T, Hashimoto T I, Kobayashi T, Murai F and Seki K 1994 *IEEE Trans. Electron Devices* **41** 1628
- [2] Schon G and Simon U 1995 *Colloid Polym. Sci.* **273** 101
- [3] Houbertz R, Feigenspan T, Mielke F, Memert U, Hartmann U, Simon U, Schon G and Schmid G 1994 *Europhys. Lett.* **28** 641
- [4] Clarke L, Wybourne M N, Yan M, Cai S X and Keana J F W 1997 *Appl. Phys. Lett.* **71** 617
- [5] Andres R P, Bein T, Dorogi M, Feng S, Henderson J I, Kubiak C P, Mahoney W, Osifchin R G and Reifenberger R 1996 *Science* **272** 1323
- [6] Brown L O and Hutchison J E 1997 *J. Am. Chem. Soc.* **119** 12384
- [7] Yan M, Cai S X, Wu J C, Duchi C A, Kanskar M, Wybourne M N and Keana J F W 1994 *Polym. Mater. Sci. Eng.* **70** 36
- [8] Schmid G 1990 *Inorg. Synth.* **27** 214
- [9] Bakhvalov N S, Kazacha G S, Likharev K K and Serdyukov S I 1989 *Sov. Phys.-JETP* **68** 581
- [10] Bakhvalov N S, Kazacha G S, Likharev K K and Serdyukov S I 1991 *Physica B* **173** 319
- [11] Geigenmuller U and Schon G 1989 *Europhys. Lett.* **10** 765
- [12] Middleton A A and Wingreen N S 1993 *Phys. Rev. Lett.* **71** 3198
- [13] Geerligs L J, Anderegg V F, Holweg P A M, Mooij J E, Pothier H, Esteve D, Urbina C and Deverot M H 1990 *Phys. Rev. Lett.* **64** 2691
- [14] Delsing P, Likharev K K, Kuzmin L S and Claeson T 1989 *Phys. Rev. Lett.* **63** 1861
- [15] Averin D V and Likharev K K 1991 *Mesoscopic Phenomena in Solids* ed B Al'tshuler, P Lee and R A Webb (Amsterdam: Elsevier)